

**Indirect transitions, free and impurity-bound excitons in gallium phosphide: A revisit with modulation and photoluminescence spectroscopy**

H. Alawadhi, R. Vogelgesang, A. K. Ramdas, T. P. Chin, and J. M. Woodall

Citation: [Journal of Applied Physics](#) **82**, 4331 (1997); doi: 10.1063/1.366241

View online: <http://dx.doi.org/10.1063/1.366241>

View Table of Contents: <http://scitation.aip.org/content/aip/journal/jap/82/9?ver=pdfcov>

Published by the [AIP Publishing](#)

---



## Re-register for Table of Content Alerts

Create a profile.



Sign up today!



# Indirect transitions, free and impurity-bound excitons in gallium phosphide: A revisit with modulation and photoluminescence spectroscopy

H. Alawadhi, R. Vogelgesang, and A. K. Ramdas  
*Department of Physics, Purdue University, West Lafayette, Indiana 47907*

T. P. Chin and J. M. Woodall  
*School of Electrical and Computer Engineering, Purdue University, West Lafayette, Indiana 47907*

(Received 28 February 1997; accepted for publication 22 July 1997)

The momentum conserving indirect excitonic transitions, from the  $\Gamma_{15}$  valence band maximum to the conduction band minima close to the  $X_1$  point in the Brillouin zone have been measured for GaP in piezo-modulated transmission. At 6 K, excitonic signatures due to phonon emission are observed at  $E_{gx} + \hbar\omega_{ph}$  for TA(X), LA(X), and TO(X) phonons ( $E_{gx}$  = free exciton band gap), whereas at 120 K signatures for both absorption and emission of LA(X) and TA(X) phonons appear. These observations yield  $E_{gx} = 2.3301(4)$  eV at 6 K. In several GaP specimens, signatures A and/or C for excitons bound to sulfur (S) and/or nitrogen (N) impurities, respectively, are observed in the piezo-modulated transmission. A parallel investigation of the spectra of recombination radiation reveals emission lines for excitons bound to S and N as well as their phonon sidebands. The phonon replicas of N consist of sharp lines in combination with the zone center optical phonons observed in the first order Raman spectrum ( $LO_{\Gamma}$  and  $TO_{\Gamma}$ ). In addition, broader replicas are observed for the A line in combination with acoustic and optical phonon branches (A-LA, A-TA, A-X). The phonon energies obtained from both piezo-modulation and photoluminescence experiments are compared with those reported in the literature. Finally, the suppression of S diffusion from a GaP substrate into a GaP epilayer achieved with an intervening GaP/AlGaP superlattice is demonstrated in both modulation and photoluminescence experiments. © 1997 American Institute of Physics.  
[S0021-8979(97)04421-6]

## I. INTRODUCTION

A number of its unique material parameters and physical characteristics singles out gallium phosphide (GaP) among the tetrahedrally coordinated III-V compound semiconductors. Its transparency in the visible led to the first study of the Raman spectrum of a semiconductor (for that matter, of any crystal) with the then relatively new lasers as monochromatic sources.<sup>1</sup> Investigations of the luminescence spectra of GaP disclosed many unique phenomena while the control of the color and efficiency of the emission with appropriate dopants made it an attractive material in the context of optoelectronics and its exploitation as light emitting diodes (LEDs).<sup>2</sup> A recent example is an acousto-phonon spectrometer utilizing nitrogen-bound excitons.<sup>3</sup> The indirect band gap, with a  $\Gamma_{15}$  valence band maximum and conduction band minima along  $\langle 100 \rangle$  close to the X points of the Brillouin zone, the latter exhibiting the so called *Camel's Back* feature;<sup>4-7</sup> the infrared<sup>8</sup> and Raman spectroscopy of phonons<sup>1,9</sup> and electronic states of donors and acceptors;<sup>10,11</sup> the application of modulation spectroscopy,<sup>12</sup> the striking donor-acceptor pair spectra literally exhibiting more than a hundred sharp lines<sup>13</sup>—these are illustrative examples of physical phenomena of basic interest, whose investigations have enriched the physics of semiconductors.

In recent years there has been a renewed interest in GaP in the context of epilayers and heterostructures. The drive for new devices like more efficient LEDs, green lasers, optical detectors and other optoelectronic devices have stimulated the development of the growth of GaP and its alloys, using techniques such as molecular beam epitaxy (MBE) and metal

organic chemical vapor deposition (MOCVD). Also, there has been a serious effort in the growth of GaP based heterostructures on the closely matched Si substrate.<sup>14,15</sup> GaP/AIP superlattices have also attracted some attention in the context of zone folding effects and the interesting possibility of a *direct* band gap structure made up of *indirect* band gap constituents.<sup>16</sup> In contrast to the extensively studied GaAs/Al<sub>1-x</sub>Ga<sub>x</sub>As multiple quantum well structures and superlattices, where the GaAs wells and AlGaAs barriers ( $x \leq 0.3$ ) have direct band gaps, both GaP wells and AIP barriers are indirect semiconductors with a band gap in the green region of the visible spectrum, and it is of interest to establish the cross-over from indirect to direct transition in these structures as a function of layer thickness.<sup>17</sup> Because of the large lattice mismatch and difference in the band gap energy between GaP and InP, GaP is also an attractive host for growing InP quantum dots and studying the effects of low dimensional confinement in such a highly strained structure.<sup>18,19</sup>

The current interest in the quantum well structures involving GaP, AIP and their alloys provides a motivation for a re-examination of the free and bound excitonic transitions and the symmetry and energy of the phonons which participate in the indirect transitions. The present investigation addresses the above considerations employing simultaneously modulated transmission and reflectivity as well as photoluminescence observed with a series of samples.

## II. EXPERIMENT

The GaP samples studied are nominally pure or deliberately doped with different levels of sulfur concentration. The

sulfur content in these samples ranged from  $2 \times 10^{16}$  to  $2 \times 10^{18} \text{ cm}^{-3}$ . In addition, GaP epilayers of  $\sim 1 \mu\text{m}$  thickness grown by MBE on undoped GaP substrates were investigated, with a GaP/AlGaP superlattice isolating the epilayer from the substrate. The estimated sulfur concentration in the epilayers was about  $5 \times 10^{15} \text{ cm}^{-3}$ . Nitrogen is not an intentional dopant and its concentration cannot be stated with confidence.

The epilayers were grown in a solid-source MBE system equipped with a valved phosphorus cracker. A small amount of white phosphorus was first converted from red phosphorus. Phosphorus tetramer molecules from the white phosphorus were then thermally cracked into dimers, which allows the safe handling of phosphorus. GaP (100) substrates were thermally cleaned at  $640^\circ\text{C}$  under phosphorus flux. GaP and AlP epilayers were grown at  $600^\circ\text{C}$ . The typical growth rate is 1 monolayer/s.

The piezo-modulated transmission measurements were performed with a Perkin Elmer (Model E1),<sup>20</sup> 0.58 m, double pass monochromator using a quartz halogen lamp as a light source and a silicon photodiode as a detector. The sample was rigidly attached to a hollow cylindrical piezoelectric transducer (PZT)<sup>21</sup> which experiences an alternating strain when excited with a 560 V, 940 Hz ac voltage. The sample was cooled in a Janis SuperTran<sup>22</sup> cryostat. Neon calibration lines were used to improve the precision in the determination of the spectral features in the piezo-modulated transmission spectra. The photoluminescence spectra were recorded with a SPEX (Model 14018) 0.85 m double grating monochromator;<sup>23</sup> the spectra were excited using the 5145, 4965, or the 4762 Å line from a Coherent Ar<sup>+</sup> laser<sup>24</sup> or the 4416 Å line from an Omnichrome He–Cd laser.<sup>25</sup> The sample was cooled to about 10 K in a Janis 10 DT cryostat and an RCA (type C31034A) photomultiplier was used as a detector.

### III. RESULTS AND DISCUSSION

#### A. Piezo-modulated transmission spectra

In Figs. 1–4, the piezo-modulated transmission spectra for four different GaP samples are displayed; in Figs. 1, 3, and 4 the temperature is 6 K, while that in Fig. 2 is 8 K. The shape of the features in these spectra provides a clue to its origin, recognizing the first derivative-like nature of the piezo-modulation spectrum. For example, the features at 2.343, 2.362, and 2.375 eV in Fig. 1 can be easily recognized as intrinsic features since in unmodulated absorption spectra they appear as *steps*, whereas with piezo-modulation they transform into *peaks*. In contrast, the sharp features at 2.309, 2.317, and 2.326 eV in Fig. 3 can all be attributed to extrinsic, impurity related, no-phonon transitions, which appear as *peaks* in the unmodulated absorption spectra.<sup>26</sup> Figure 1 corresponds to a nominally undoped, *n*-type substrate with an unintentional sulfur concentration of  $2 \times 10^{16} \text{ cm}^{-3}$ . Hence the intrinsic features are relatively strong, while the extrinsic feature at 2.309 eV is barely visible. In contrast, the intrinsic features become relatively weak with an increase in the doping level of impurities as seen in Figs. 2, 3, and 4. On the basis of such piezo-modulated transmission spectra of sev-

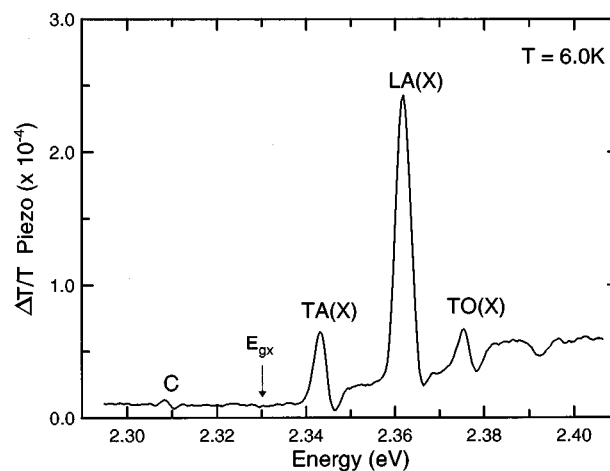


FIG. 1. Piezo-modulated transmission spectrum of an “undoped” GaP substrate. At 6 K the signatures corresponding to the creation of free excitons, assisted by the wave vector conserving phonons with wave vectors close to the X point of the Brillouin zone, are observed. The free exciton energy determined from this study is labeled  $E_{gx}$ . The small signature labeled C is due to S-bound excitons indicating the presence of S at doping level of  $10^{16} \text{ cm}^{-3}$ .

eral doped and undoped GaP samples, we have established a correlation between the strength of the extrinsic lines and the concentration of sulfur and nitrogen in the sample. The doping levels of sulfur and nitrogen in these samples indicate that the feature at 2.317 eV is related to substitutional isoelectronic nitrogen, while the features at 2.309 eV and 2.326 eV are related to substitutional sulfur, a neutral donor.

The lowest band edge in GaP corresponds to the indirect transitions from the  $\Gamma_{15}$  valence band maximum to the lowest equivalent conduction band minima near  $X_1$  (Ref. 27); from a critical analysis of the photoluminescence data, Dean and Herbert<sup>5</sup> concluded that the conduction band minima of GaP lie at  $0.953 k_{(100)}^{\text{max}}$ . Conservation of wave vector  $\mathbf{k}$  in the optical transition is ensured by the emission or absorption of

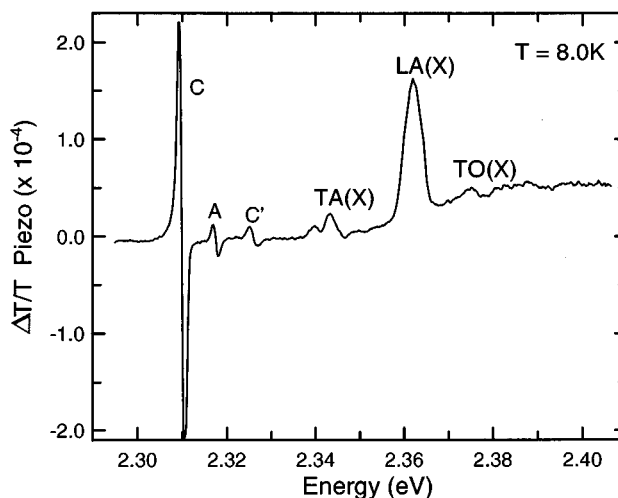


FIG. 2. Piezo-modulated transmission spectrum of S-doped GaP, showing a large signature labeled C, ascribed to S-bound excitons, as well as a relatively smaller signature (A) of excitons bound to nitrogen in the nominally N-free sample. C' is attributed to the first excited state of the S-bound exciton. The nominal sulfur concentration is  $\sim 10^{17} \text{ cm}^{-3}$ .

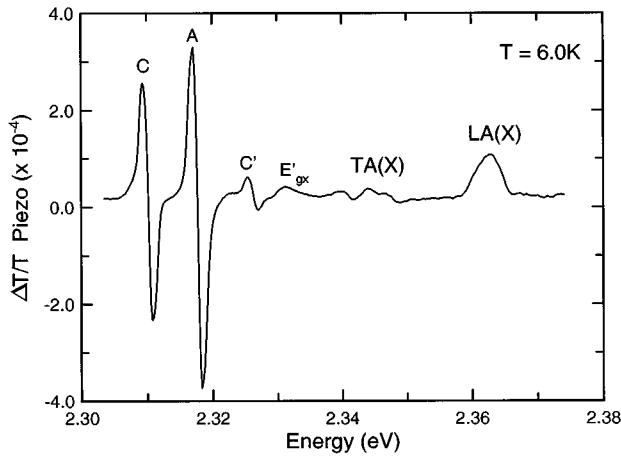


FIG. 3. Piezo-modulated transmission spectrum of heavily S- and N-doped GaP, exhibiting large signals of excitons bound to impurities. The signature at  $E'_{gx}$  is due to free excitons, i.e., without phonon emission, being allowed by the partial loss of translational symmetry due to the presence of isoelectronic N. The nominal sulfur concentration is  $\sim 10^{17} \text{ cm}^{-3}$ .

acoustic and optical phonons having a wave vector  $\mathbf{q}$  close to the X point. The interband, or equivalently, the free excitonic transitions occur in piezo-modulated transmission spectra at  $E_{gx} \pm \hbar\omega_{ph}$  (plus for phonon emission and minus for phonon absorption). Here  $E_{gx}$  is the exciton energy and  $\hbar\omega_{ph}$  is the relevant phonon energy. Choosing the P atom as the origin, the LO, TO, LA and TA phonons in GaP, with  $\mathbf{q}$  vectors corresponding to the X point, have  $X_3$ ,  $X_5$ ,  $X_1$  and  $X_5$  symmetries, respectively.<sup>28</sup> The symmetry of a phonon involved in an indirect transition depends on the symmetry of the intermediate electronic state (this virtual transition to the intermediate state does not conserve energy—although it has to conserve wave vector as a result of crystal translation symmetry). Therefore, transitions via the lowest conduction band at  $\Gamma$  (symmetry  $\Gamma_1$ ) involve only phonons of symmetry  $X_1$ , namely the LA phonons. Those mediated by the  $\Gamma_{15}$  conduction band minima involve LO, TO and TA phonons, whereas all four phonons can participate in the transitions via the  $X_5$  valence band minima. Since the energy denominator

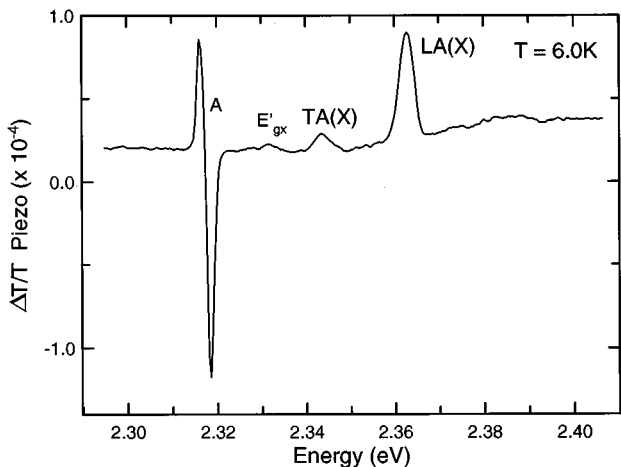


FIG. 4. The piezo-modulated transmission spectrum of N-doped GaP showing a large signal for N-bound excitons.

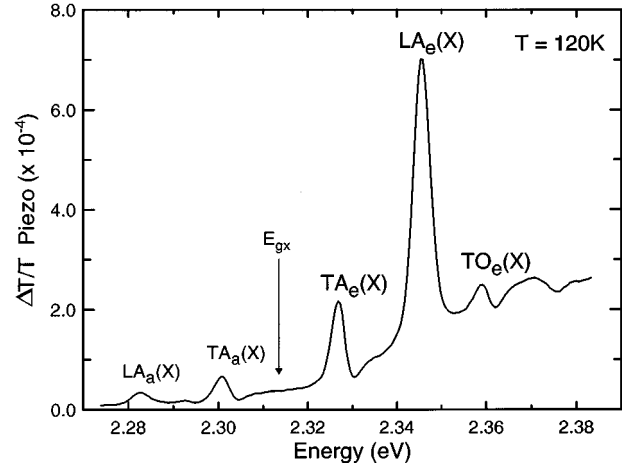


FIG. 5. Piezo-modulated transmission of the same sample as in Fig. 1 but at a higher temperature of 120 K. At this temperature the zone boundary LA(X) and TA(X) phonons are sufficiently populated to allow a simultaneous observation of the wave vector conserving free excitonic signatures associated with the creation as well as annihilation of the phonons, labeled with subscripts e and a, respectively.

in the transition probability for the process with the  $\Gamma_1$  intermediate state is much smaller than those involving  $\Gamma_{15}$  or  $X_5$ , the LA assisted transitions are expected to be the strongest phonon assisted transitions.<sup>29</sup> Here an implicit assumption is made that the 5% departure of the  $|\mathbf{k}|$  of the conduction band minima from  $X_1$  is not significant for the  $\mathbf{k}$  selection rule. On this basis, the strong peak that appears at 2.362 eV in the spectra of all the samples is attributed to the LA(X) phonon assisted transition. Consistent with the phonon energies deduced from inelastic neutron scattering,<sup>30</sup> the feature at 2.343 eV is attributed to the TA(X) assisted transition. Based on the energies of the TO(X) and LO(X) given by inelastic neutron scattering<sup>30</sup> (45.6 meV and 46.8 meV, respectively) and the width of the signature, the feature at 2.375 eV cannot be uniquely assigned to an excitonic transition assisted by one or the other optical phonon. However, Dean and Thomas<sup>31</sup> have estimated that the intensity of the TO(X) assisted transition is an order of magnitude larger than that assisted by LO(X). On this basis the feature is ascribed to TO(X).

As all the above measurements were performed at low temperatures, the indirect transitions are excitonic in nature and  $\mathbf{k}$ -conservation involves only the emission of phonons. Features corresponding to the indirect transitions assisted by the absorption of phonons appear distinctly at temperatures exceeding 50 K; a typical spectrum at 120 K for the undoped sample is shown in Fig. 5. The positions of the excitonic transitions associated with phonon absorption ( $E_{gx} - \hbar\omega_{ph}$ ), labeled with subscript a, in combination with those associated with phonon emission ( $E_{gx} + \hbar\omega_{ph}$ ), labeled with subscript e, offer a convenient and accurate method for determining energies of both the exciton and the phonons at that temperature. Indeed,  $\hbar\omega_{ph}$  is just half the difference between the energies of the phonon-assisted transitions involving the emission and absorption of that phonon species. It was also found that, within the experimental errors in our measurements (not presented here), the phonon energies thus de-

TABLE I. Energies of the indirect exciton, the associated phonons, and the transition energies of nitrogen-bound and sulfur-bound excitons.

	Piezo (6 K)	Luminescence and Raman (6 K)	Ref. 12 (1.6 K)	Ref. 32 ( $\leq 25$ K)	Ref. 31 (1.6 K)
$E_{gx}$ (eV)	2.3301(4)		2.333		2.329(1)
TA(X) (meV)	13.1(2)		13(1)	13.1(1)	12.8(5)
LA(X) (meV)	31.5(2)		32(1)	31.5(1)	31.5(5)
TO(X)/LO(X) (meV)	45.0(3)		44(1)	45.9(1)	46.5(10)
TO( $\Gamma$ ) (meV)		45.3(1)	42.2(2)	45.2(1)	
LO( $\Gamma$ ) (meV)		50.1(1)		50.1(1)	
“X” (meV)		48.3(1)		48.9(2)	
$E_{gx}(N)$ (eV)	2.3172(2)	2.3173(1): A 2.3163(1): B			
$E_{gx}(S)$ (eV)	2.3094(2)	2.3097(1): C		2.30955(10)	

duced do not show any observable change in the range of  $50 \text{ K} \leq T \leq 120 \text{ K}$ . Therefore, the energies of the LA and TA phonons deduced from Fig. 5 were used, along with the low temperature data in Fig. 1, to obtain  $E_{gx}$  for GaP at 6 K. Dean and Thomas<sup>31</sup> followed this approach in their analysis of the intrinsic absorption edge where *steps* are observed corresponding to the thresholds of the different phonon-assisted transitions. We emphasize the advantage of piezomodulation of the transmission spectrum in the indirect transition range with absorption coefficients less than  $100 \text{ cm}^{-1}$ . The modulation technique ignores the featureless monotonous increase of absorption, leaving only the distinct maxima corresponding to the thresholds. Finally, the binding energies of excitons bound to nitrogen isoelectronic traps [ $E_{gx} - E_{gx}(N)$ ], and sulfur neutral donors [ $E_{gx} - E_{gx}(S)$ ], were deduced from the positions of the nitrogen-bound and sulfur-bound excitonic signatures in Figs. 2, 3, and 4 at  $E_{gx}(N)$  and  $E_{gx}(S)$ , respectively, together with the value for  $E_{gx}$ . In Table I, our values of  $E_{gx}$ ,  $E_{gx}(N)$  and  $E_{gx}(S)$  are compared with those from Refs. 12, 31, and 32.

For the samples with a strong N-bound excitonic signature, a feature was observed in their modulation spectra, at an energy close to, but above the expected free excitonic band gap. In Fig. 3 this feature appears at  $E'_{gx} = 2.3306 \text{ eV}$ , about  $0.5 \text{ meV}$  above  $E_{gx}$ ; its strength is strongly correlated with that of the N-bound exciton (A-line) suggesting its association with the presence of N.<sup>33</sup> Substitution of P atoms with N perturbs the translational symmetry of the lattice and hence allows the no-phonon free exciton transition which would otherwise be forbidden. It is interesting to speculate whether the  $0.5 \text{ meV}$  shift in energy above  $E_{gx}$  can be attributed to the GaP being an incipient “alloy” with a small fraction of GaN ( $E_g = 3.5 \text{ eV}$ ). Mobsby *et al.*<sup>34</sup> have made a similar observation in the change of GaP band gap involving As.

For the heavily S-doped samples, besides the no-phonon C line at  $2.3094 \text{ eV}$ , a second weaker feature  $C'$  at  $2.3255 \text{ eV}$  is observed in the modulation spectra, as seen in Figs. 2 and 3. This feature is attributed to the first excited state of the S-bound excitons.<sup>32</sup> With this interpretation and a simple hydrogenic model for the bound exciton, the difference in the energies between  $C'$  and C yields  $(3/4)(E_{gx} - E_C)$ ; the value of  $E_{gx}$  thus deduced is  $2.3309 \text{ eV}$ , in good agreement with

$2.3301(4) \text{ eV}$  obtained from the phonon assisted, free excitonic features discussed earlier.

## B. Photoluminescence spectra

As discussed above, the excitonic transition from the valence band maximum to the conduction band minima near X in pure GaP at low temperatures occurs at  $E_{gx} + \hbar\omega_{ph}$  in piezo-modulated transmission spectrum. In contrast, the excitonic recombination following the excitation with a photon energy much larger than that of the indirect energy gap, followed in turn by thermalization, occurs at  $E_{gx} - \hbar\omega_{ph}$ , again with phonon emission for  $\mathbf{k}$  conservation. The phonon-assisted excitonic features in photoluminescence and in piezo-modulated transmission, *both* recorded at low temperatures, should thus make their appearance as mirror images in energy with respect to  $E_{gx}$ . It is therefore of interest to record the excitonic signatures in this manner and deduce  $E_{gx}$  as well as  $\omega_{ph}$  from such a study as was indeed accomplished by Parks *et al.*<sup>35</sup> for monoisotopic Ge.

Motivated by this approach, we measured the spectra of the recombination radiation for the samples used for piezomodulated transmission. Figure 6 shows the photoluminescence spectrum for the same sample as that studied in Fig. 1. As can be seen, *no* signatures were observed at  $2.3169$ ,  $2.2985$ , and  $2.285 \text{ eV}$  expected for TA(X), LA(X), and TO(X) phonon-emission-assisted free excitonic transitions. In contrast, distinct peaks appear at  $2.3173 \text{ eV}$  and  $2.3097 \text{ eV}$ , consistent with the positions for excitons bound to N (labeled A and B) and to S (labeled C), respectively. In piezo-modulated transmission, the phonon-assisted free excitonic transitions manifest themselves in a pronounced manner, whereas the S-bound excitonic signature is barely noticed and the N-bound excitonic feature is below detection. It is clear that, after the free excitons are created, they are rapidly captured by the N and S impurities, followed by the observed radiative decay. In Fig. 7 the features in photoluminescence and the corresponding signatures in piezomodulated transmission associated with excitons bound to S and N can be easily seen. At lower energies the photoluminescence spectrum also shows signatures of the donor-acceptor pair recombination involving S donors and carbon

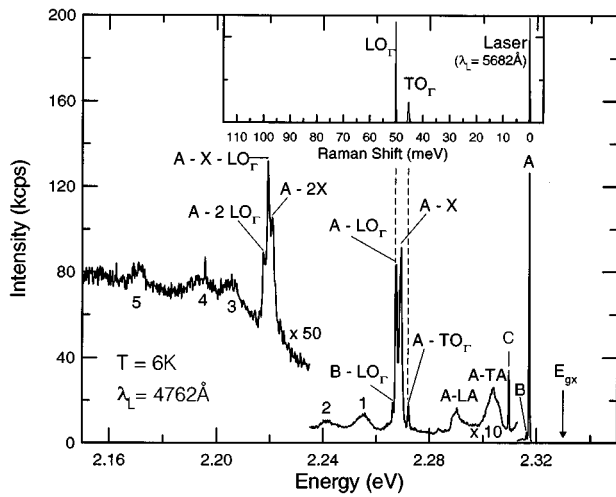


FIG. 6. Photoluminescence spectrum of a GaP sample similar to that used in Fig. 1. The inset shows the first order Raman spectrum excited with  $\lambda_L = 5682 \text{ \AA}$   $\text{Kr}^+$  radiation and displayed with an energy scale identical to that used for the main figure and  $\hbar\omega_L$  shifted to match the energy of the A line.

acceptors.<sup>36</sup> In Fig. 8(a) the photoluminescence spectrum of a GaP substrate is shown where S-related features are stronger than those associated with N. It should be noted that all these aspects are strongly dependent on the *extrinsic* properties of GaP.

It is well known that the recombination radiation spectrum of a semiconductor exhibits signatures associated with excitons trapped at defect centers; the energy positions of such *bound excitonic* (BE) transitions allow one to deduce the binding energies referred to that of the free excitons (FE). Among the impurities in GaP known to produce bound excitons, sulfur and nitrogen are the most common.<sup>37</sup> Whereas the nitrogen bound exciton shows a splitting into lines A and B due to the spin-spin interaction of the electrons and holes, their relative intensity being strongly temperature

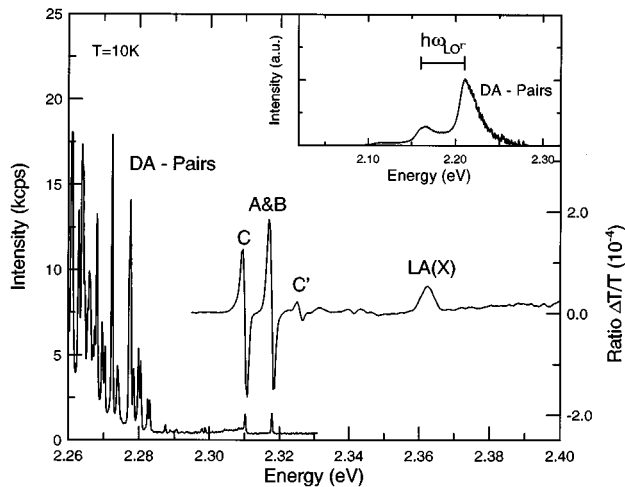


FIG. 7. Piezo-modulated transmission and photoluminescence spectra, of the sample used in Fig. 3, compared to show the signature for S-bound and N-bound excitons in both; the characteristic DA pair spectra and its  $\text{LO}_{\Gamma}$ -assisted satellites are displayed. The photoluminescence was excited with the  $4965 \text{ \AA}$  line of the  $\text{Ar}^+$  laser.

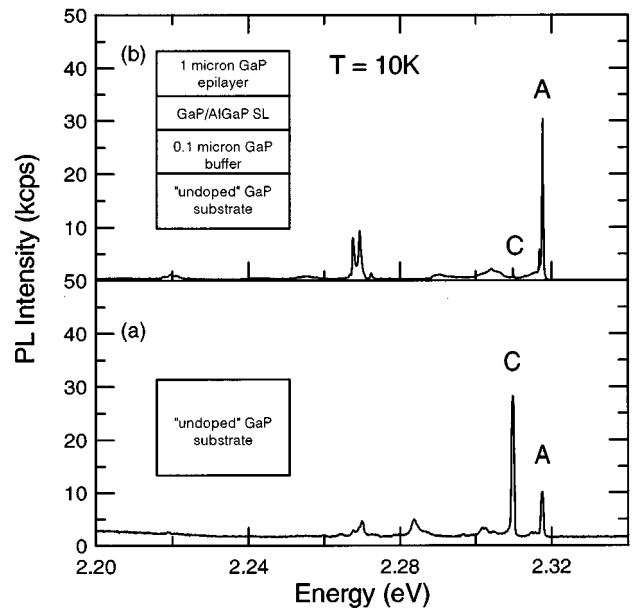


FIG. 8. The S signature in the photoluminescence spectrum of a nominally undoped GaP substrate (a) and its suppression in a GaP epilayer separated from the underlying GaP substrate by a GaP/AlGaP superlattice and GaP buffer layer (b). The spectra were excited with the  $4416 \text{ \AA}$  line of the HeCd laser; the larger background in (a) is due to the five times larger power (50 mW) compared to that in (b).

dependent,<sup>37</sup> the exciton bound to neutral sulfur always appears as a single line C. While phonon replicas appear distinctly for the A and B lines, such signatures are very weak for the C line, even in heavily S-doped specimens we have studied (spectra not presented). This has been attributed to C resulting from excitons weakly bound to a shallow, neutral donor, whereas A and B arise from excitons bound to an isoelectronic, isolated N.<sup>38</sup> Two of the replicas occur at energies consistent with electronic transitions accompanied by zone-center optical phonons with energies  $50.1 \text{ meV}$  ( $\text{LO}_{\Gamma}$ ) and  $45.3 \text{ meV}$  ( $\text{TO}_{\Gamma}$ ). The inset to Fig. 6 shows the Raman spectrum of the same sample displayed on the same energy scale, the energy of the exciting laser radiation ( $\hbar\omega_L = 2.183 \text{ eV}$ ) from a  $\text{Kr}^+$  laser being aligned with that of line A in the photoluminescence spectrum. The association of the phonon replicas of A in combination with  $\text{LO}_{\Gamma}$  and  $\text{TO}_{\Gamma}$  is underscored by dashed lines.

Other photoluminescence signatures, however, could not be conclusively attributed to single phonon modes. In the context of the features located at  $48.3 \text{ meV}$  (X),  $\sim 12.5 \text{ meV}$  (TA) and  $\sim 22.5 \text{ meV}$  (LA) below A, Zhang *et al.*<sup>39</sup> have recently made a careful analysis of alternate models proposed for the underlying electron-phonon interaction. One model assumes momentum conservation (MC) during the interaction, whereas the other appeals to the "configuration coordinate" (CC) picture in order to interpret the phonon sidebands. Zhang *et al.* conclude that the former is appropriate for shallow donors and acceptors, such as S and Mg, while the CC model is more relevant for excitons bound to isoelectronic impurities like N. On the basis of the CC model, features labeled TA and LA are ascribed to the A transitions accompanied by transverse and longitudinal acoustic phonon emissions, respectively. The origin of the X

line is ascribed to the A transition in combination with the LO phonon branch, the peak reflecting the one-phonon density of states. Other labels in Fig. 6 are based on the assignments for A and B transitions accompanied with  $LO_{\Gamma}$ ,  $TO_{\Gamma}$ , X, TA, LA and their combinations/overtones. Lines 1 and 2 are in turn acoustic phonon replicas of  $(A-TO_{\Gamma})$ ,  $(A-X)$ ,  $(A-LO_{\Gamma})$  and  $(B-LO_{\Gamma})$ , whereas 3 and 4 are associated with acoustic phonon replicas of  $(A-2X)$ ,  $(A-X-LO_{\Gamma})$  and  $(A-2LO_{\Gamma})$  and 5 with their optical phonon replicas.

In heavily N-doped GaP specimens, excitons bound to pairs of nitrogen atoms, located sufficiently close to each other, have been reported; they give rise to a series of discrete NN lines according to the possible discrete internuclear distances.<sup>38</sup> As mentioned earlier, heavily doped GaP samples may give rise to the so-called *donor-acceptor* (DA) pair spectra. More than 100 separate lines have been resolved at low temperatures and low excitation power densities.<sup>13,40</sup> They are produced by pairs of donors and acceptors, separated by discrete distances according to the possible locations consistent with the zinc-blende lattice geometry of GaP. The distance-dependent, Coulomb-like interaction between a donor and an acceptor then gives rise to the discrete series of lines observed in Fig. 7.

### C. Out-diffusion of sulfur in MBE growth

The presence of S and N, which enter the crystals during crystal growth as unintended dopants, has prevented the observation of the phonon assisted free excitonic signatures in the photoluminescence spectra and frustrated the deduction of  $E_{gx}$  from a comparison of such a signature with that in the piezo-modulated transmission spectra. Attempts to observe the free excitonic signatures in a presumably pure epilayer grown on a GaP substrate by MBE also failed. It has been conjectured<sup>41</sup> that S present in a GaP substrate might out-diffuse into a GaP epilayer grown on it. In addition, both piezo-modulated transmission and luminescence do not discriminate between the signatures which originate in an epilayer and those from the substrate. As a strategy to inhibit the possible out-diffusion of S from the substrate as well as to achieve optical isolation, heterostructures were fabricated with MBE in which the final epilayer is “shielded” from the underlying GaP substrate by

- (a) a GaP/ $Al_{0.2}Ga_{0.8}P$  superlattice consisting of 20 50-Å-thick alternate layers and
- (b) a “Bragg stack” consisting of 15 alternate layers of 398-Å-thick  $Al_{0.5}Ga_{0.5}P$  and 363-Å-thick GaP.

In both cases, the heterostructures were grown on the substrate with an intervening buffer of GaP. In Fig. 8(b) the luminescence spectrum from an epilayer fabricated with an intervening superlattice indeed showed a significantly diminished C line compared to that from the bare substrate on which the heterostructure was grown [Fig. 8(a)]; this suggests a much reduced S concentration in the epilayer. The N signature (A line), however, shows an increase with respect to that in the bare substrate; it appears that the increase is due to the residual  $N_2$  in the growth chamber. The piezo-modulated *transmission* spectrum of a heterostructure [Fig. 9(a)] consisting of a GaP epilayer grown on a “Bragg stack”

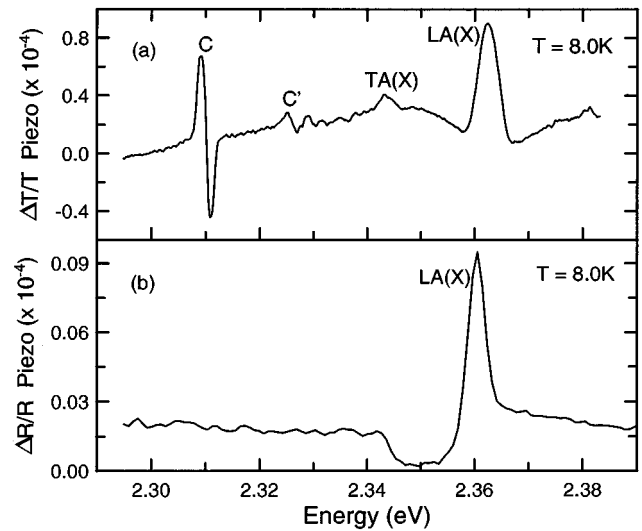


FIG. 9. (a) The piezo-modulated transmission spectrum through a pure GaP epilayer separated from the underlying S-doped substrate by a Bragg stack. The strong S signature is attributed to the substrate. (b) The piezo-modulated transmission of the epilayer only, observed in the reflecting geometry, by a double traversal through the epilayer and a reflection at the Bragg stack. Note the absence of the S signature.

shows the S signatures (C and C') as well as TA(X) and LA(X). In a dramatic contrast, the piezo-modulated spectrum recorded in the *reflection* geometry [Fig. 9(b)] displays only the LA(X), the strongest phonon-assisted excitonic signature, with no hint of C and C'. It must be emphasized that in the reflection geometry employed, one in reality observes the “transmission” of the epilayer only, thanks to the return of the transmitted light by reflection from the underlying Bragg stack. When the piezo-modulated reflectivity is recorded from the substrate side, the  $(\Delta R/R)$  versus photon energy did reveal the presence of S as in Fig. 1, the substrate being from the same parent material. These facts of observation clearly demonstrate that C and C' originate in the substrate and any out-diffusion of S into the epilayer has been successfully prevented by the superlattice (Bragg stack) and/or by the GaP buffer layer. Our experiments do not reveal whether the prevention of out-diffusion has been accomplished by the heterostructure or by the buffer alone or by their combination; the former is needed for optical isolation, whereas the buffer layer is essential for the heterostructure growth.

### IV. CONCLUDING REMARKS

The objective of the present investigation was to *simultaneously* observe the phonon assisted free excitonic transitions in photoluminescence and in absorption, as revealed sensitively in piezo-modulated transmission. As noted, the modulated transmission of specimens relatively free from S and N did reveal strong signatures at  $E_{gx} + \hbar\omega_{ph}$ , but we were unsuccessful in observing their mirror images at  $E_{gx} - \hbar\omega_{ph}$  in photoluminescence. Instead, we observed signatures of excitons bound to S and/or N as well as their phonon replicas. However, the free excitonic signatures, observed in piezo-modulated transmission for  $E_{gx} - \hbar\omega_{ph}$  at elevated temperatures and the phonon replicas

of bound excitons in photoluminescence did allow the determination of  $E_{gx}$  and  $\hbar\omega_{ph}$ . It appears that free excitons, once created, are rapidly captured nonradiatively by the intentional dopants like S or the unintentional dopants like isoelectronic N. The state-of-the-art for bulk crystal growth of pure GaP has yet to reach the status attained in that of Si, Ge and GaAs.

Our attempts to fabricate pure GaP epilayers on GaP substrate (with MBE) also did not enable us to observe free excitonic signatures in luminescence. The relatively high transparency in the spectral range in which the phonon-assisted indirect transitions occur also implied that the substrate is inevitably probed in piezo-modulated transmission. In addition, out-diffusion of S from the substrate into the epilayer is a distinct possibility. The “optical isolation” of the epilayer from the substrate by an intervening heterostructure did demonstrate that the strategy is effective in establishing that a S-free epilayer can be grown on a GaP substrate even if the latter is not free from S. The alternative approach,<sup>14,15</sup> in which a GaP epilayer is grown on the closely lattice matched Si substrate, is clearly of interest in this context.

## ACKNOWLEDGMENTS

The authors acknowledge support from the National Science Foundation: Materials Research Science and Engineering Center Grant Nos. DMR94-00415 and DMR93-03186 (AKR).

<sup>1</sup>M. V. Hobden and J. P. Russell, Phys. Lett. **13B**, 39 (1964).

<sup>2</sup>A. A. Bergh and P. J. Dean, Proc. IEEE **60**, 156 (1972).

<sup>3</sup>T. Bouma and J. I. Dijkhuis, Appl. Phys. Lett. **63**, 3429 (1993).

<sup>4</sup>P. Lawaetz, Solid State Commun. **16**, 65 (1975).

<sup>5</sup>P. J. Dean and D. C. Herbert, J. Lumin. **14**, 55 (1976).

<sup>6</sup>M. Capizzi, F. Evangelisti, P. Fiorini, A. Frova, and F. Patella, Solid State Commun. **24**, 801 (1977).

<sup>7</sup>R. G. Humphreys, U. Rössler, and M. Cardona, Phys. Rev. B **18**, 5590 (1978).

<sup>8</sup>D. A. Kleinman and W. G. Spitzer, Phys. Rev. **118**, 110 (1960).

<sup>9</sup>B. A. Weinstein and M. Cardona, Phys. Rev. B **8**, 2795 (1973).

<sup>10</sup>D. D. Manchon and P. J. Dean, in *10th International Conference on the Physics of Semiconductors* (United States Atomic Energy Commission, Oakridge, TN, 1970), p. 760.

<sup>11</sup>A. Onton and R. C. Taylor, Phys. Rev. B **1**, 2587 (1970).

<sup>12</sup>D. Auvergne, P. Merle, and H. Mathieu, Phys. Rev. B **12**, 1371 (1975).

<sup>13</sup>J. J. Hopfield, D. G. Thomas, and M. Gershenson, Phys. Rev. Lett. **10**, 162 (1963).

<sup>14</sup>T. Soga, T. Jimbo, and M. Umeno, Appl. Phys. Lett. **63**, 2543 (1993).

<sup>15</sup>Y. V. Zhilyaev, V. V. Krivolapchuk, N. Nazarov, I. P. Nikitina, N. K. Poletaev, D. V. Sergeev, V. V. Travnikov, and L. M. Fedorov, Sov. Phys. Semicond. **24**, 819 (1990).

<sup>16</sup>K. Asami, H. Asahi, T. Watanabe, M. Enokida, S. Gonda, and Sg. Fujita, Appl. Phys. Lett. **62**, 81 (1993).

<sup>17</sup>M. Kumagai, T. Takagahara, and E. Hanamura, Phys. Rev. B **37**, 898 (1988).

<sup>18</sup>S. P. DenBaars, C. M. Reaves, V. Bressler-Hill, S. Varma, W. H. Weinberg, and P. M. Petroff, J. Cryst. Growth **145**, 721 (1994).

<sup>19</sup>N. Carlsson, W. Seifert, A. Petersson, P. Castrillo, M. E. Pistol, and L. Samuelson, Appl. Phys. Lett. **65**, 3093 (1994).

<sup>20</sup>Perkin Elmer Corporation, 761 Main Ave., Norwalk, CT 06859.

<sup>21</sup>Piezokinetics Inc., P.O. Box 756, Bellefonte, PA 16823.

<sup>22</sup>Janis Research Inc., P.O. Box 696, 2 Jewel Dr., Wilmington, MA 01887-0696.

<sup>23</sup>SPEX Industries Inc., 3880 Park Ave., Metuchen, NJ 08840.

<sup>24</sup>Coherent Inc., 5100 Patrick Henry Dr., P.O. Box 54980, Santa Clara, CA 95054.

<sup>25</sup>Omnichrome, 13620 5th St., Chino, CA 91710.

<sup>26</sup>See J. Camassel, D. Auvergne, H. Mathieu, and B. Pistoulet, Phys. Status Solidi **42**, 147 (1970) for an illuminating discussion on the nature of the piezo-modulation spectra.

<sup>27</sup>J. R. Chelikowsky and M. L. Cohen, Phys. Rev. B **14**, 556 (1976), see p. 566, Fig. 7.

<sup>28</sup>J. L. Birman, Phys. Rev. **131**, 1489 (1963).

<sup>29</sup>P. Y. Yu and M. Cardona, in *Fundamentals of Semiconductors* (Springer, New York, 1996), p. 262, Eq. (6.61).

<sup>30</sup>J. L. Yarnell, J. L. Warren, R. G. Wenzel, and P. J. Dean, in *Neutron Inelastic Scattering Symposium* (International Atomic Energy Agency, Vienna, 1968), Vol. 1, p. 301.

<sup>31</sup>P. J. Dean and D. G. Thomas, Phys. Rev. **150**, 690 (1966).

<sup>32</sup>P. J. Dean, Phys. Rev. **157**, 655 (1967).

<sup>33</sup>J. J. Hopfield, P. J. Dean, and D. G. Thomas, Phys. Rev. **158**, 748 (1967).

<sup>34</sup>C. D. Mobsby, E. C. Lightowers, and G. Davies, J. Lumin. **4**, 29 (1971).

<sup>35</sup>C. Parks, A. K. Ramdas, S. Rodriguez, K. M. Itoh, and E. E. Haller, Phys. Rev. B **49**, 14244 (1994).

<sup>36</sup>P. J. Dean and L. Patrick, Phys. Rev. B **2**, 1888 (1970). The positions and the relative intensities of the lines in the pair spectra match closely with those in spectrum simulated with S donors and C acceptors. See Fig. 5, p. 1893.

<sup>37</sup>D. G. Thomas, M. Gershenson, and J. J. Hopfield, Phys. Rev. **131**, 2397 (1963).

<sup>38</sup>D. G. Thomas and J. J. Hopfield, Phys. Rev. **150**, 680 (1966). These authors have made a careful analysis of the intensity of the absorption and fluorescence due to the transitions associated with excitons bound to isolated N and NN pairs. This analysis enabled them to put an upper limit on the N concentration; when it is exceeded, NN lines appear. According to P. J. Wiesner, R. A. Street, and H. D. Wolf, Phys. Rev. Lett. **35**, 1366 (1975), this upper limit is  $\sim 2 \times 10^{17} \text{ cm}^{-3}$ .

<sup>39</sup>Y. Zhang, W. Ge, M. D. Sturge, J. Zheng, and B. Wu, Phys. Rev. B **47**, 6330 (1993).

<sup>40</sup>P. J. Dean, in *Progress in Solid State Chemistry*, edited by J. O. McCaldin and G. Somorjai (Pergamon, Oxford, 1973), Vol. 8, pp. 1–126.

<sup>41</sup>H. E. Ruda, L. Jedral, and L. Mannik, Phys. Rev. B **44**, 8702 (1991).